S & M 4225

Incremental Conductance Method with Intelligence Predication for Maximum Power Point Tracking of Photovoltaic Module Array

Kuei-Hsiang Chao, 1* Thi Thanh Truc Bau, 2 and Tsai-Hsun Chu1

¹Department of Electrical Engineering, National Chin-Yi University of Technology
 No. 57, Sec. 2, Zhongshan Rd., Taiping Dist., Taichung 41170, Taiwan
 ²Graduate Institute, Prospective Technology of Electrical Engineering and Computer Science,
 National Chin-Yi University of Technology, Taichung 41170, Taiwan

(Received September 17, 2025; accepted November 7, 2025)

Keywords: photovoltaic module array, maximum power point tracking, power–voltage characteristic curve, modified incremental conductance method, performance of tracking response

In this paper, a method based on modified incremental conductance with intelligence predication was proposed as an application on a photovoltaic module array (PVMA) for the purpose of maximum power point tracking (MPPT), which served to improve the power generation performance of PVMA. Since PVMA is affected by solar irradiance and temperature change, the output maximum power point (MPP) changes accordingly. In addition, owing to the fixed length of tracking pace for the conventional incremental conductance method (ICM), the time required for tracking MPP may take longer. Therefore, the modified ICM with step size predication was proposed in this paper. The length of tracking pace could automatically adapt to the gradient of the power-voltage characteristic curve for PVMA. The 0.8 times voltage for the MPP of PVMA under standard test conditions would serve as the initial voltage for MPPT, which would be utilized to increase the output power of PVMA. In this study, the 62050H-600S programmable DC power supply produced by Chroma ATE Inc. was applied to simulate the output characteristics of a 4-series-3-parallel PVMA. In contrast, the conventional and modified ICMs were applied for MPPT purposes. The actual test results proved that the modified ICM proposed in this paper provided a better response in terms of both tracking speed and steadystate performance than the conventional ICM under different solar conditions.

1. Introduction

Along with the continuous increase in the awareness of climate change and environmental protection globally, using photovoltaic power generation systems as a clean and renewable energy format has attracted increasing attention. However, with the progressive severity of global warming, the enhancement of power generation efficiency with photovoltaic power generation systems has become a pressing issue. Among photovoltaic power generation systems, the maximum power point tracking (MPPT) is a critical technology that mainly focuses on maximizing the output power of photovoltaic module arrays (PVMAs). As the application of

*Corresponding author: e-mail: chaokh@ncut.edu.tw

https://doi.org/10.18494/SAM5938

photovoltaic power generation systems continues to expand, the research and application of MPPT technology have been valued progressively. Conventional MPPT methods include the perturb and observe method, (1-3) incremental conductance method (ICM), (4-6) power feedback method,⁽⁷⁾ and constant voltage method.⁽⁸⁾ However, these methods can only achieve good tracking performance under specific solar and temperature conditions. Among them, the advantages of a conventional ICM are simple structure, ease of implementation, lower cost, and fast-tracking response. The algorithm is simple and easy to understand and implement, and requires no complex calculations or controllers. Moreover, the hardware cost is relatively low, making it suitable for low-cost applications. However, under fixed working conditions, the conventional ICM can ensure stable system operation and achieve fundamental MPPT. In practical applications nevertheless, the conventional ICM may present certain shortages such as poor adaptability to environmental changes and slower convergence. Therefore, the modification of the conventional ICM to improve its MPPT performance has become one of the key items among researchers in photovoltaic power generation systems. In addition, more advanced approaches have also been developed, such as fuzzy logic algorithm^(9,10) and particle swarm optimization, (11,12) which are capable of providing improved global tracking performance under partial shading or rapidly changing irradiance conditions. However, these methods must choose the appropriate iteration constant. Otherwise, it may cause system instability, and the operation is complicated.

On the basis of the above, the modified ICM with a change in pacing length was proposed in this paper for the MPPT of PVMA. This allowed higher self-adaptability, faster convergence, better stability, and stronger scalability. Furthermore, the power generation performance of the photovoltaic power generation system can be enhanced effectively. Therefore, the objective of this study was to explore the MPPT technology with ICM under variable pacing lengths. First, the initial voltage of MPPT was set at 0.8 times the MPPT voltage for PVMA under standard test conditions (STCs) and served as the starting voltage for tracking. At the same time, a better response was achieved in terms of both tracking speed and steady-state performance.

2. Architecture of MPPT for PVMA

The module adopted in this paper for the 4-series-3-parallel PVMA was a Kyocera KS20 photovoltaic module produced by Kyocera Corporation in Japan. (13) The specifications are shown in Table 1. The simulation results of current-voltage (I-V) and power-voltage (P-V) characteristic curves of the Kyocera KS20 photovoltaic module with solar irradiance at 500 and 1000 W/m², respectively, are shown in Fig. 1.

Table 1
Specifications of Kyocero KS20 photovoltaic module. (13)
Open-circuit voltage (V_{oc}) 21.5 V
Short-circuit current (I_{sc}) 1.24 A
Voltage at maximum power point (V_{mp}) 16.9 V
Current at maximum power point (I_{mp}) 1.2 A
Maximum power (P_{mp}) 20.28 W

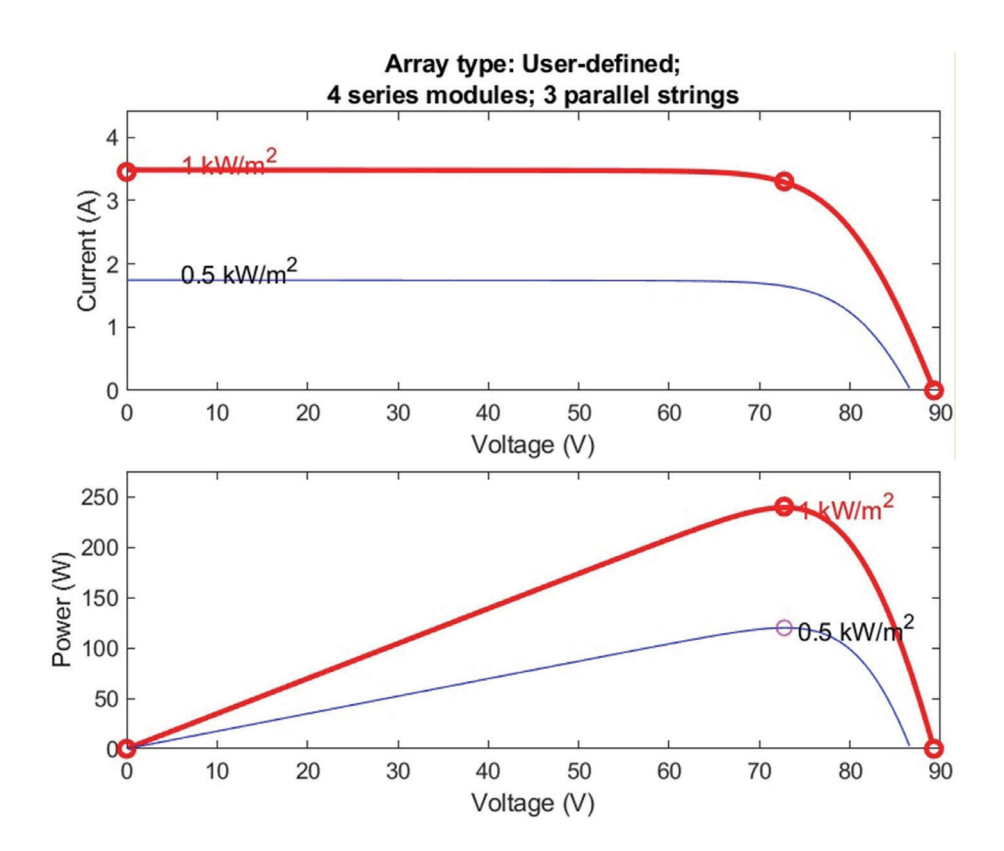


Fig. 1. (Color online) Simulation results of P-V and I-V characteristic curves for photovoltaic module.

The architecture of MPPT mentioned in this paper is shown in Fig. 2, which mainly consisted of boost converter circuits^(14,15) and a modified ICM controller. By controlling the on-off duration of the power semiconductor switch of the boost converter, the MPPT of PVMA was implemented.

3. Boost Converter Design

Figure 3 shows the architecture of the boost converter circuit. The circuit structure consisted of fast diodes, a power inductor, filter capacitors, and a switch, where the switch on-off function is controlled by pulse width modulation. Prior to the circuit analysis, five assumptions were made as below: (1) The circuit was operating under a steady state; (2) the switch cycle was defined as T, the switch on-time as DT, and the switch off-time as (1 - D)T. Among them, D was the duty cycle defined as $D = t_{on}/T$, while t_{on} was the switch-on duration in one cycle; (3) the inductor current was operating in continuous conduction mode; (4) the capacitance was extremely large, making the output voltage V_o constant; and (5) all circuit components were ideal.

Equation (1) can be derived according to the volt-second balance of the storage inductor L.⁽¹⁶⁾

$$V_o = \frac{V_s}{1 - D} \tag{1}$$

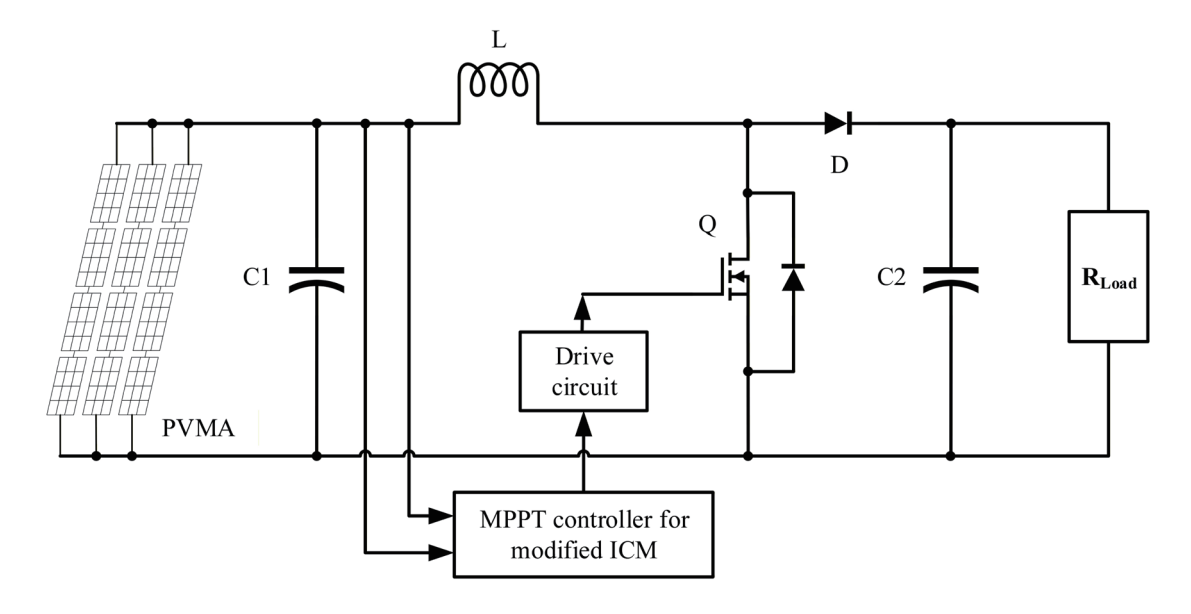


Fig. 2. Architecture of MPPT system with modified ICM.

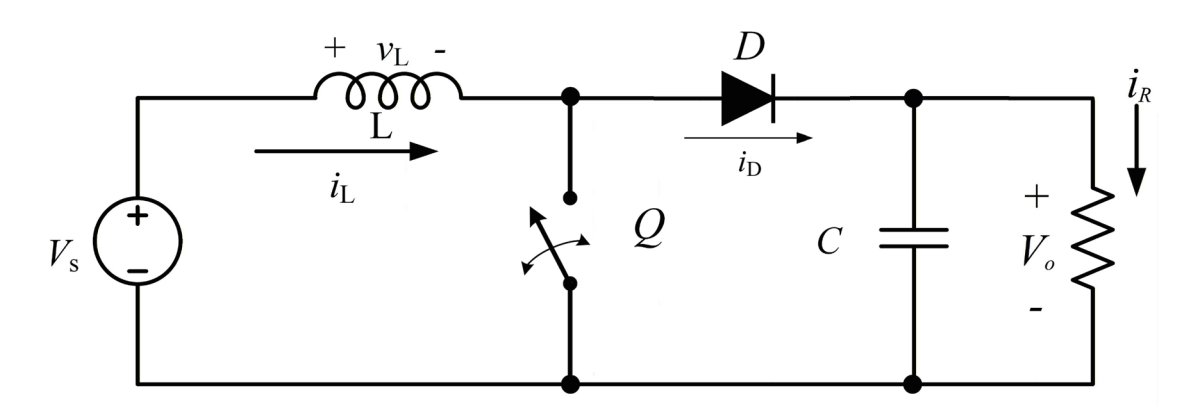


Fig. 3. Architecture of boost converter circuit.

Among them, V_o was the output voltage, V_s was the input voltage, and D was the duty cycle. Since the duty cycle satisfies 0 < D < 1, the input voltage V_s is less than the output voltage V_o , which confirms that the converter operates as a boost converter.

When the boost converter is operated at a higher switch frequency, the volume of the power inductor and filter capacitor can be reduced. Therefore, 25 kHz was used as the switch frequency of the boost converter in this paper. After calculation, the boost converter's inductance and capacitance can be derived, (16) and the specifications of relevant components are shown in Table 2.

4. Incremental Conductance Method of MPPT

ICM is a common technique used for MPPT in photovoltaic systems. By monitoring the voltage and current of PVMA, the method calculates the dynamic (i.e., the rate of change in

Table 2 Component specifications for boost converter. (16)

1 1			
Components	Specifications		
Filter capacitor C_1	220 μF, withstand voltage at 400 V		
Filter capacitor C_2	470 μF, withstand voltage at 450 V		
Power inductor L	1.67 mH, withstand current 7.4 A		
Fast diode D	Withstand voltage 600 V,		
Diode IQBE60E60A1	withstand current 60 A		
Switch Q IREP460B	Withstand voltage 500 V,		
	withstand current 20 A		

current against voltage) and static conductance values to confirm the maximum power point (MPP). The equivalence between the dynamic and static conductance values represented that PVMA was operating at MPP. ICM is the MPPT technique extensively applied with excellent performance. The features include high efficiency, fast response, good stability, and simple implementation.

4.1 Conventional ICM

Such ICM utilizes the rate of change dP/dV in output power and voltage of the photovoltaic module array as zero at MPP to serve as the basis for determination; thus,

$$\frac{dP}{dV} = \frac{d(IV)}{dV} = I + V\frac{dI}{dV} = 0.$$
 (2)

From Eq. (2), Eq. (3) can be derived as

$$\frac{dI}{dV} = -\frac{I}{V}. (3)$$

Among them, $G_s \triangleq -I/V$ was the static conductance and $G_d \triangleq dI/dV$ was the dynamic conductance. The dynamic conductance being higher than the static conductance indicated that the current work point is on the left of MPP. Hence, the duty cycle for the converter needs to be reduced, so that the work point can shift to MPP on the right. Alternatively, the dynamic conductance being lower than the static conductance indicated that the current work point is on the right of MPP. Hence, the duty cycle for the converter needs to be increased, so that the work point can shift to MPP on the left until the dynamic conductance is equivalent to the static conductance, reflecting that the MPP has been tracked. The working characteristics are shown in Fig. 4. Figure 5 shows the flow chart of MPPT for PVMA utilizing ICM.

4.2 ICM with fixed initial tracking voltage

To improve the tracking speed of the conventional ICM, a fixed voltage was utilized as the initial tracking voltage V_{start} for the improvement of the conventional ICM. V_{start} was set at 0.8

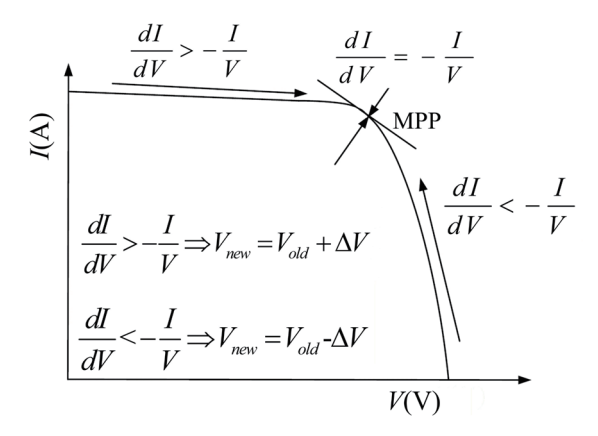


Fig. 4. Working characteristics of ICM.

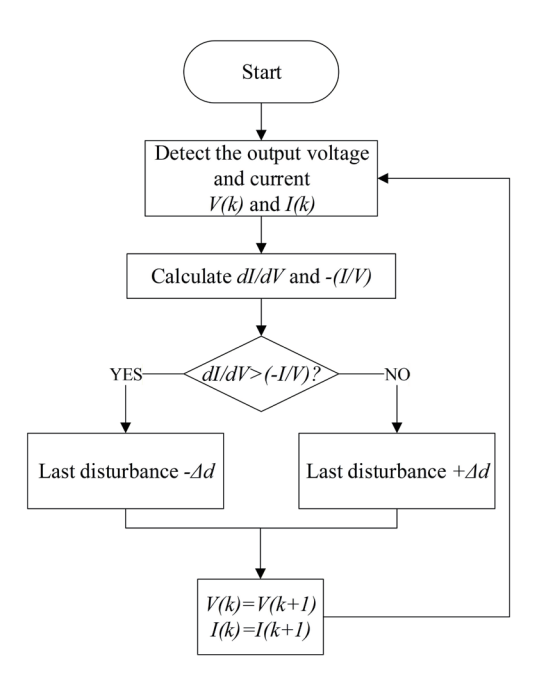


Fig. 5. Flow chart of ICM.

times the MPP voltage V_{mp} for PVMA, i.e., $V_{start} = 0.8V_{mp}$; thus, each tracking starts from V_{start} . From that, the modified ICM with fixed initial tracking voltage can track MPP faster.

4.3 ICM with fixed initial tracking voltage and adjusted pacing length at the same time

Although ICM with fixed initial tracking voltage provided higher tracking speed, the same duty cycle variation was still adopted as the pacing length for tracking. If the pacing length was set too little, the tracking speed of the system would be affected. However, if the pacing length was set too large, the tracking time could be reduced, but there would be extensive oscillation near MPP and power loss. Thus, to improve system stability and reduce oscillation amplitude, as

well as shorten the time required for tracking MPP, a fixed initial tracking voltage at $0.8V_{mp}$ was proposed in this paper. In addition, automatic adjustment on the variation of the duty cycle according to the work point was also proposed, so the variation of the duty cycle decreased when the work point became closer to MPP, i.e., the pacing length decreased. When the work point moved further away from MPP, the variation of the duty cycle increased, i.e., the pacing length increased.

Figure 6 shows the illustration of a modified ICM with pacing length for tracking (i.e., the variation of duty cycle) automatically adjusted according to the gradient of the P-V characteristic curve. Among them, m was the gradient of the P-V characteristic curve, (17) which was defined as

$$m_{k+1} = \frac{P_{k+1} - P_k}{V_{k+1} - V_k} \,. \tag{4}$$

Therefore, besides setting the initial tracking voltage to 0.8 times the MPP voltage V_{mp} for PVMA under STC, the duty cycle variation Δd is also adaptively regulated in accordance with Eq. (5).

$$\Delta d_{k+1} = 5 \times 10^{-3} \times |m_{k+1}| \tag{5}$$

The gradient m greater than zero indicated tracking the left of MPP. Then, the tracking should be directed to MPP on the right. The gradient m less than zero indicated tracking the right of MPP. Then, the tracking should be directed to MPP on the left. When MPP and the gradient m were closer to zero, the variation Δd was also closer to zero.

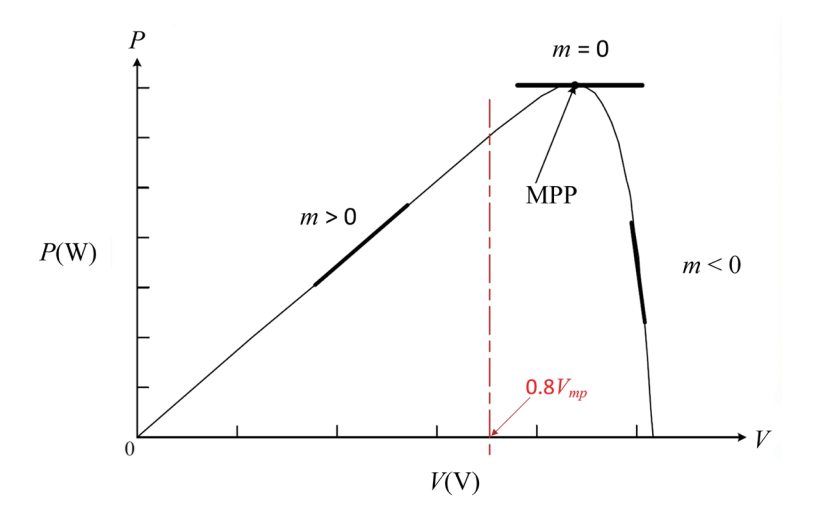


Fig. 6. (Color online) Illustration for gradient of *P–V* characteristic curve.

5. Actual Test Results

The 62050H-600S programmable DC power supply produced by Chroma ATE Inc. was used to simulate the output characteristics of the 4-series-3-parallel PVMA, while three different methods were used for actual tests on MPPT. The ambient temperature was maintained at 25 ± 2 °C, and irradiance profiles were reproduced according to STC. Voltage and current were sampled at 25 kHz with resolutions of 0.01 V and 0.01 A using a digital oscilloscope and a data acquisition system. The measurement uncertainties of voltage and current sensors were within $\pm 1\%$. These conditions ensured that the experimental results were both accurate and reproducible. Figures 7 and 8 show the measured I-V and P-V characteristic curves from the actual test on the 4-series-3-parallel PVMA, respectively. For the actual hardware circuit to implement MPPT, the software

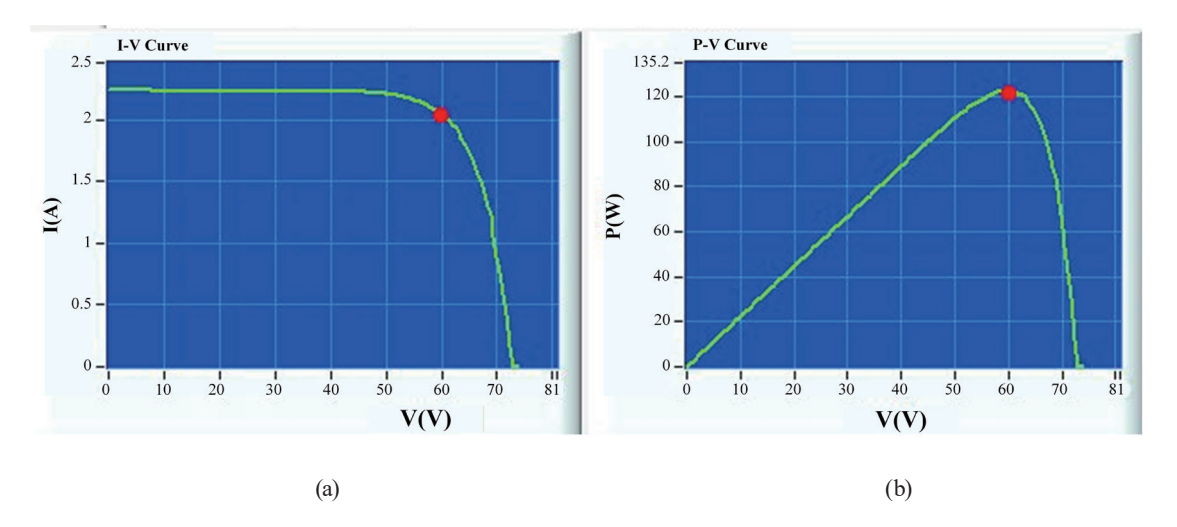


Fig. 7. (Color online) I-V and P-V characteristic curves from actual test on the 4-series-3-parallel PVMA under solar irradiance at 500 W/m².

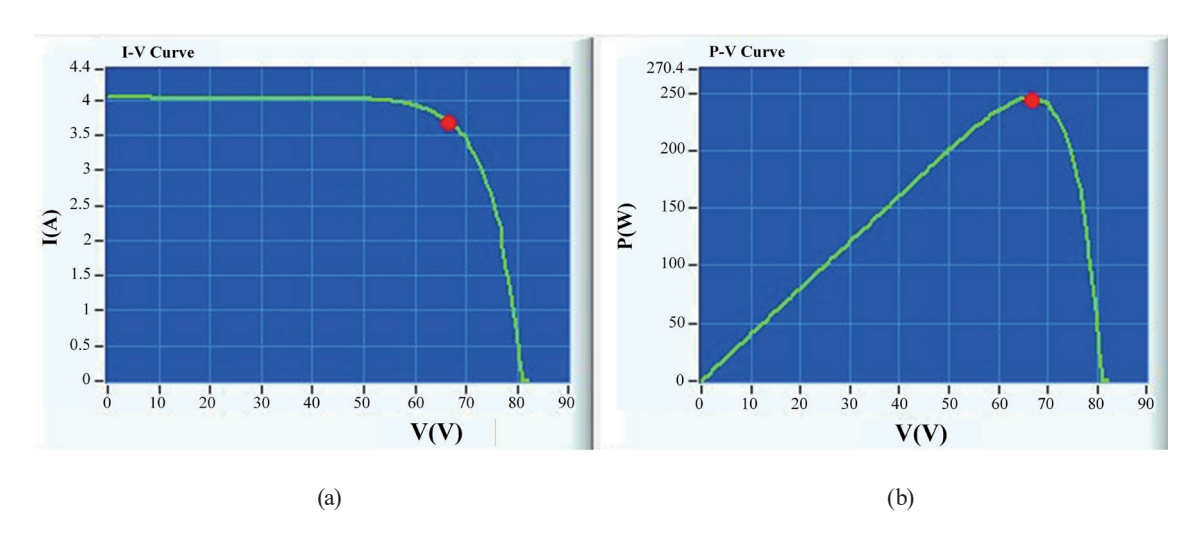


Fig. 8. (Color online) I-V and P-V characteristic curves from actual test on the 4-series-3-parallel PVMA under solar irradiance at 1000 W/m².

"Altium Designer" was used to complete the wiring and component configuration. The appearance of the hardware circuit is shown in Fig. 9.

First, the actual test on MPPT was carried out with the conventional and modified ICMs. Figures 10 to 12 show the results from the actual test utilizing the conventional ICM, the ICM with fixed initial tracking voltage, and the ICM with fixed initial tracking voltage together with

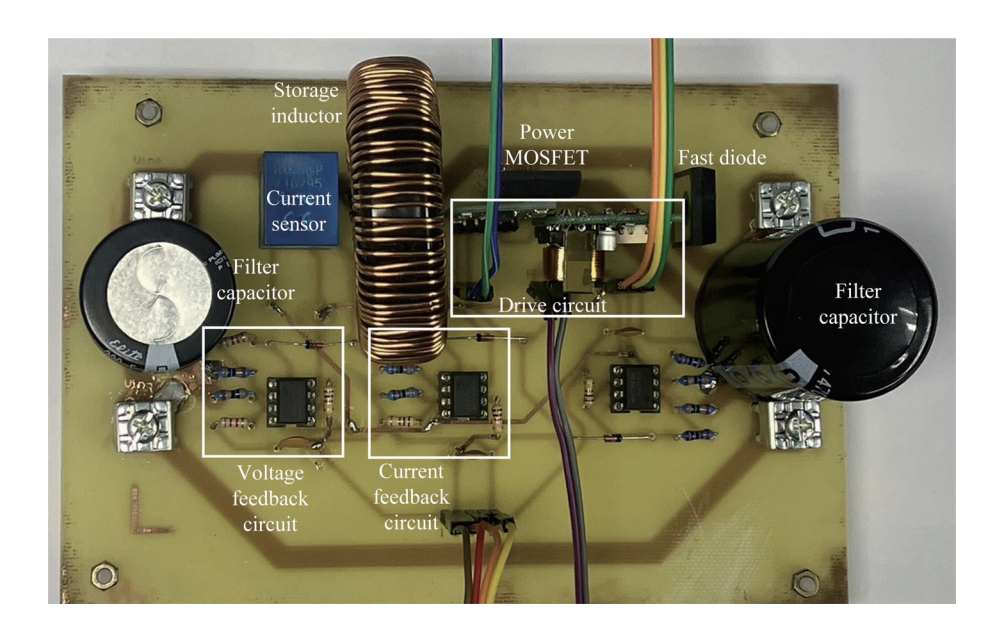


Fig. 9. (Color online) Appearance of actual hardware circuit.

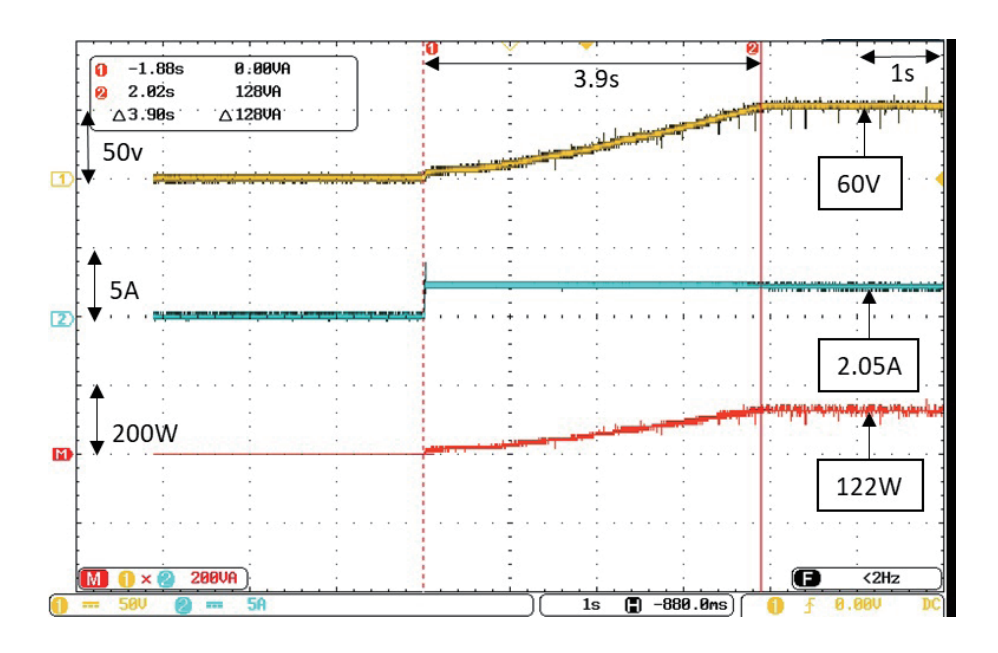


Fig. 10. (Color online) Actual test results of MPPT utilizing conventional ICM under solar irradiance at 500 W/m 2 and temperature of 25 °C.

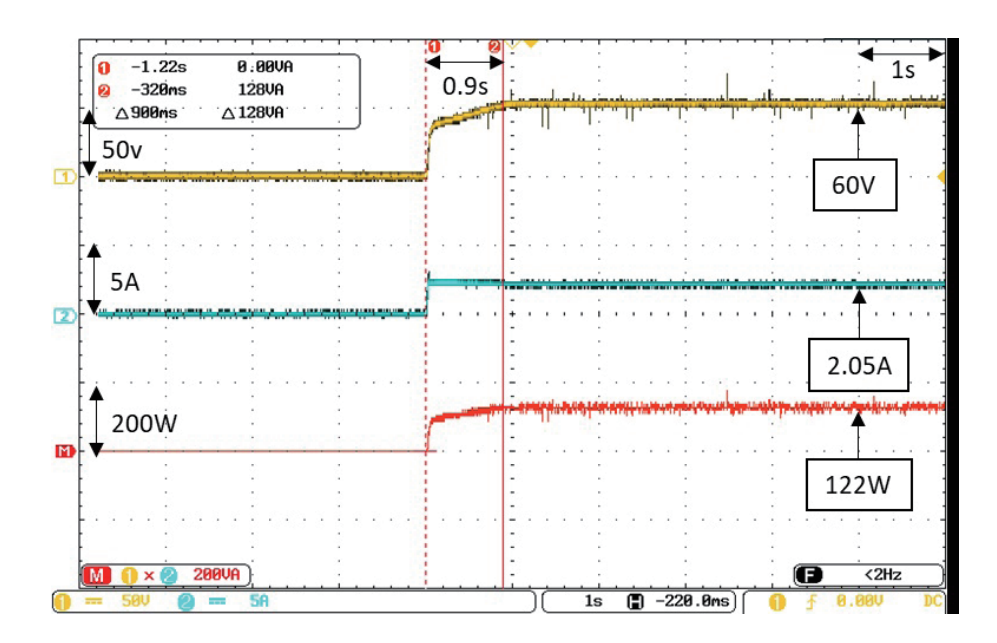


Fig. 11. (Color online) Actual test results of MPPT utilizing modified ICM with fixed initial tracking voltage under solar irradiance at 500 W/m² and temperature of 25 °C.

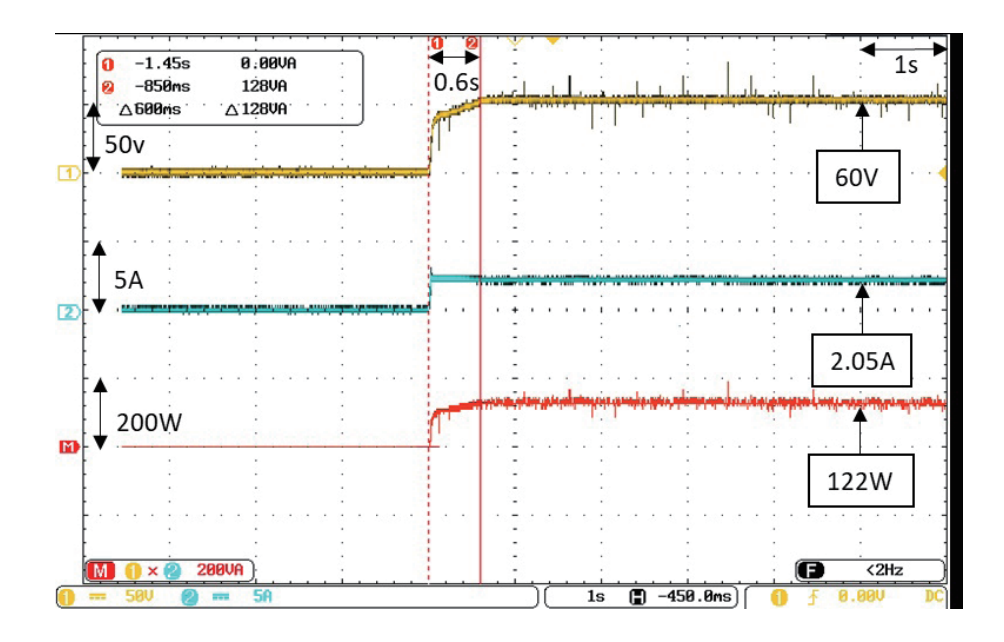


Fig. 12. (Color online) Actual test results of MPPT utilizing ICM with fixed initial tracking voltage together with adjusted pacing lengths under solar irradiance at 500 W/m^2 and temperature of $25 \text{ }^{\circ}\text{C}$.

adjusted pacing lengths under solar irradiance at 500 W/m² and a temperature of 25 °C, respectively. Figures 13 to 15 show the results from the actual test utilizing the conventional ICM, the ICM with fixed initial tracking voltage, and the ICM with fixed initial tracking voltage together with adjusted pacing lengths under solar irradiance at 1000 W/m² and a temperature of 25 °C, respectively.

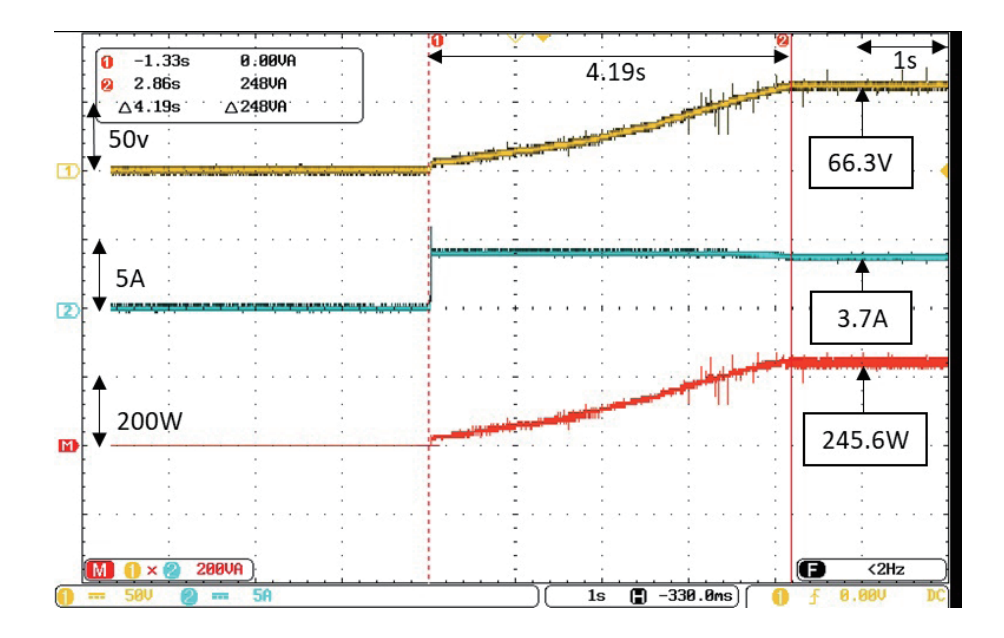


Fig. 13. (Color online) Actual test results of MPPT utilizing conventional ICM under solar irradiance at 1000 W/m² and temperature of 25 °C.

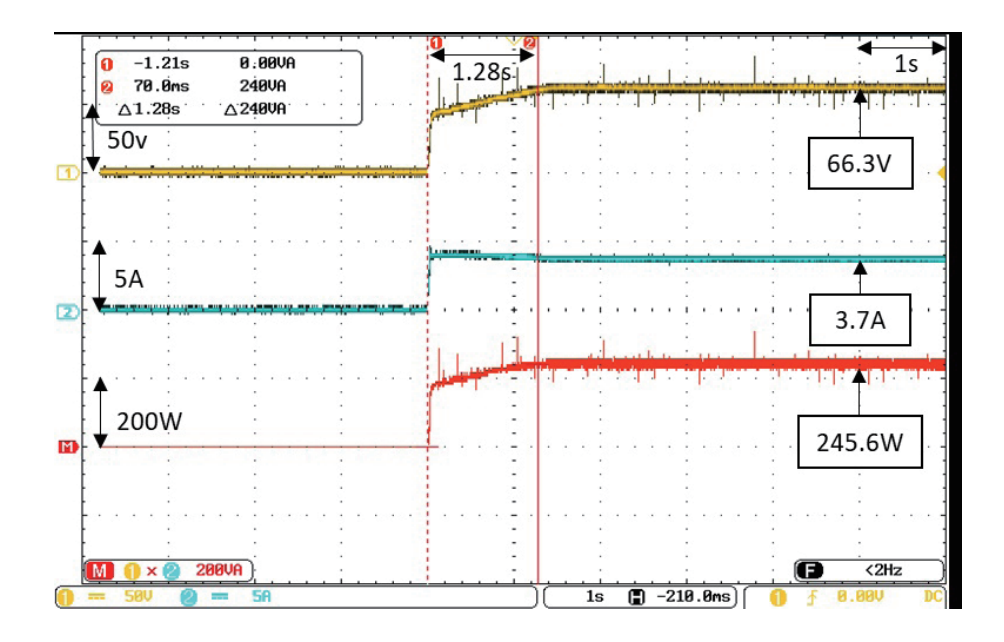


Fig. 14. (Color online) Actual test results of MPPT utilizing modified ICM with fixed initial tracking voltage under solar irradiance at 1000 W/m^2 and temperature of 25 °C.

The actual test results indicated that under solar irradiance at 500 W/m², all three tracking methods can track MPP at 122 W, together with the MPP voltage at 60 V and the MPP current at 2.05 A. However, the duration required for the conventional ICM tracking of MPP was 3.9 s, whereas the modified ICM with fixed initial tracking voltage only took 0.9 s for tracking MPP. On the other hand, the tracking duration required for ICM with a fixed initial tracking voltage together with adjusted pacing lengths decreased significantly to 0.6 s.

Similarly, under solar irradiance at 1000 W/m², all three methods can track MPP at 245.6 W, together with the MPP voltage at 66.3 V and the MPP current at 3.7 A. However, the duration of tracking MPP utilizing the conventional ICM was 4.19 s, whereas the duration of tracking MPP utilizing ICM with the fixed initial tracking voltage was reduced to 1.28 s, and the ICM with the fixed initial tracking voltage together with adjusted pacing lengths took only 0.8 s for tracking MPP. Therefore, the actual test results proved that both modified ICMs proposed took less time for tracking MPP than the conventional ICM under different solar irradiances. In particular, ICM with the fixed initial tracking voltage together with adjusted pacing lengths did not only provide faster dynamic response, but also higher performance in the steady-state response. From the above, utilizing the modified ICM for tracking MPP of PVMA could achieve higher power generation efficiency.

Table 3 shows a performance comparison between the conventional and proposed ICMs under different irradiance conditions.

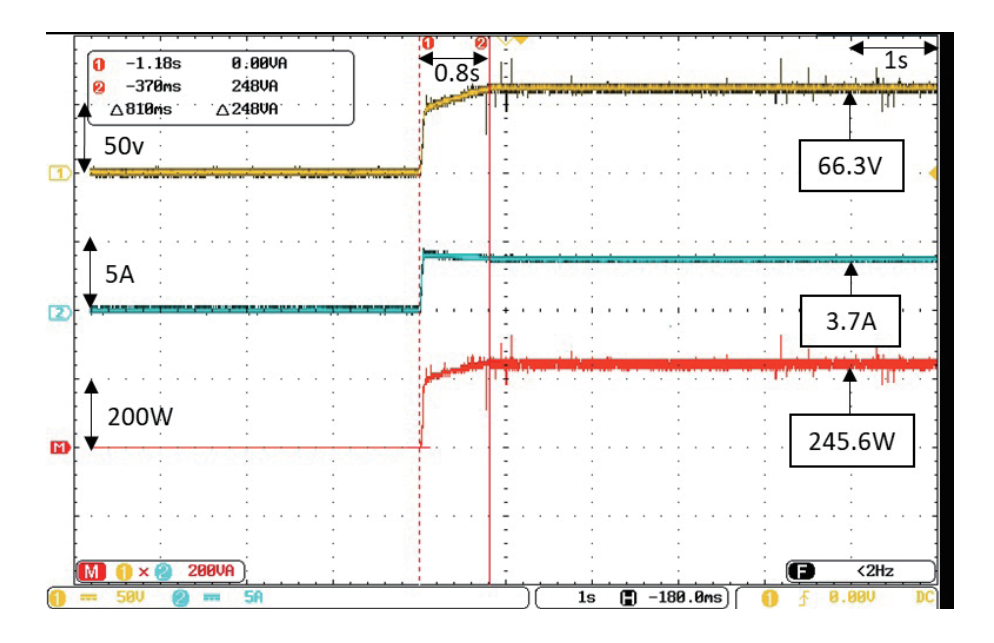


Fig. 15. (Color online) Actual test results of MPPT utilizing ICM with fixed initial tracking voltage together with adjusted pacing lengths under solar irradiance at 1000 W/m² and temperature of 25 °C.

Table 3
Performance comparison between conventional and proposed ICMs under different irradiance conditions.

Irradiance (W/m ²)	Method	Tracking time (s)	Efficiency (%)	Power ripple (%)
500	Conventional ICM	3.9	91.3	2.1
	Modified ICM	0.9	91.3	2.1
	(fixed $V_{start} = 0.8V_{mp}$)			
	Modified ICM	0.6	92.0	1.0
	(fixed V_{start} + adaptive pacing)			
1000	Conventional ICM	4.19	91.5	2.5
	Modified ICM	1.28	91.4	2.5
	(fixed $V_{start} = 0.8V_{mp}$)			
	Modified ICM	0.8	92.2	0.8
	(fixed V_{start} + adaptive pacing)			

6. Conclusions

In this paper, two modified ICMs were proposed for the MPPT of PVMA to enhance the tracking performance. By setting the initial tracking voltage of the conventional ICM at 0.8 times the MPP voltage for PVMA under STC, as well as utilizing the gradient of the P-Vcharacteristic curve produced from PVMA as the basis of adjusting pacing lengths for tracking simultaneously, practical application was made to PVMA for MPPT. The modified ICMs proposed in this paper included the ICM with fixed initial tracking voltage and the ICM with fixed initial tracking voltage together with pacing lengths adjusted according to the gradient of the P-V characteristic curve. Among them, the ICM with fixed initial tracking voltage together with pacing lengths adjusted according to the gradient of the P-V characteristic curve provided an optimal response in terms of tracking speed. The modified ICMs proposed not only provided a better response in terms of tracking speed than the conventional ICM but also proved from actual test results that, upon the variation of solar irradiance, the modified ICMs can promptly track MPP under changing solar conditions. With the addition of pacing lengths for tracking adjusted according to the gradient of the P-V characteristic curve, such a method can also reduce the amplitude of oscillation after tracking MPP, which enhanced the tracking performance under the steady state.

Acknowledgments

This work was supported by the National Science and Technology of Council, Taiwan, under Grant no. NSTC 113-2221-E-167-035-.

References

- 1. F. Raziya, M. Afnaz, S. Jesudason, I. Ranaweera, and H. Walpita: Proc. Moratuwa Engineering Research Conf. (2019) 474–479. https://doi.org/10.1109/MERCon.2019.8818684
- 2 M. W. Dzulqarnain, K. Lian, Suwarno, A. A. Subaktiar, Z. Fan, and K. Jen: Proc. Int. Conf. International Conference on Power Engineering and Renewable Energy (2024) 1–6. https://doi.org/10.1109/ICPERE63447.2024.10845676
- 3 S. Fang, L. Wang, C. Zeng, P. Li, X. He, and C. Ma: Proc. Int. Conf. Automation, Robotics and Computer Engineering (2024) 458–462. https://doi.org/10.1109/ICARCE63054.2024.00093
- 4 S. Lakshminarayanan, H. D. Kattimani, and P. A. Athavale: Proc. Int. Conf. Computing for Sustainability and Intelligent Future (2025) 1–6. https://doi.org/10.1109/COMP-SIF65618.2025.10969962
- 5 S. A. Mohammadi, S. H. Fathi, H. Goudarzhagh, and S. Heidarbozorg: Proc. Power Electronic and Drive Systems and Technologies Conf. (2025) 1–6. https://doi.org/10.1109/PEDSTC65486.2025.10912013
- 6 H. Suryoatmojo, R. M. Hakim, D. C. Riawan, R. Mardiyanto, S. Anam, and E. Setijadi: Proc. Int. Seminar on Intelligent Technology and Its Applications (2019) 108–113. https://doi.org/10.1109/ISITIA.2019.8937264
- 7 Y. Yusong, E. Solomin, and W. Lei: Proc. Int. Conf. Industrial Engineering, Applications and Manufacturing (2020) 1–6. https://doi.org/10.1109/ICIEAM48468.2020.9112043
- 8 G. Luo, J. Liu, T. Yang, Y. Dou, and N. Chen: Proc. China Int. SAR Symp. (2022) 1–6. https://doi.org/10.1109/CISS57580.2022.9971405
- 9 R. K. Rai and O. P. Rahi: Proc. Int. Conf. Electrical, Electronics, Information and Communication Technologies (2022) 1–5. https://doi.org/10.1109/ICEEICT53079.2022.9768650
- 10 D. Reddy, V. Kulkarni, and S. Ramaswamy: Proc. Int. Conf. Intelligent and Innovative Technologies in Computing, Electrical and Electronics (2023) 375–379. https://doi.org/10.1109/IITCEE57236.2023.10091023
- 11 X. Li, Z. Youzhuo, H. Wei, Z. Shuyi, Z. Wenqiang, and C. Haobin: Proc. Asia Conf. Power and Electrical Engineering (2024) 2348–2352. https://doi.org/10.1109/ACPEE60788.2024.10532728

- 12 M. M. Shehu, M. Dong, and J. Hu: Proc. IEEE Conf. Industrial Electronics and Applications (2021) 267–272. https://doi.org/10.1109/ICIEA51954.2021.9516360
- 13 Kyocera KS20 Solar Panel, Specifications: https://www.ecodirect.com/Kyocera-KS20-Solar-Panel-20-Watt-12-Volt-p/kyocera-ks20.htm (accessed December 2024).
- V. K. Bandaru, A. Kotapati, P. Seelam, and S. P. Edara: Proc. Int. Conf. Power Electronics Converters for Transportation and Energy Applications (2025) 1–6. https://doi.org/10.1109/PECTEA61788.2025.11076324
- 15 I. E. Haji, K. Mustapha, A. Elhasnaoui, and S. Sahbani: Proc. Int. Conf. Power and Energy Technology (2023) 102–106. https://doi.org/10.1109/ICPET59380.2023.10367717
- 16 D. W. Hart: Introduction to Power Electronics (Pearson Book Company, 2002) 2nd ed.
- 17 T. T. T. Bau and K. H. Chao: Sens. Mater. **35** (2023) 2637. https://doi.org/10.18494/SAM4353

About the Authors



Kuei-Hsiang Chao received his B.S. degree in electrical engineering from National Taiwan Institute of Technology, Taipei, Taiwan, in 1988, and his M.S. and Ph.D. degrees in electrical engineering from National Tsing Hua University, Hsinchu, Taiwan, in 1990 and 2000, respectively. He is presently a tenured distinguished professor at National Chin-Yi University of Technology, Taichung, Taiwan. His areas of interest are computer-based control systems, applications of control theory, renewable energy, and power electronics. Dr. Chao is a life member of the Solar Energy and New Energy Association and a member of the IEEE.



Thi Thanh Truc Bau received her B.S. and M.S. degrees in electrical engineering from National Chin-Yi University of Technology, Taichung, Taiwan, in 2022 and 2024, respectively. She is currently pursuing her Ph.D. degree at National Chin-Yi University of Technology, Taichung, Taiwan. Her main research interests include power electronics technology, maximum power point tracking (MPPT) for photovoltaic module arrays, and fault diagnosis.



Tsai-Hsun Chu received her B.S. degree in electronic engineering from Feng Chia University, Taichung, Taiwan, in 2015. She is now studying for a master's degree in National Chin-Yi University of Technology, Taichung, Taiwan. Her areas of interest are power electronics and maximum power point tracking for a photovoltaic module array.